

# Prospecting for Zoonotic Pathogens by Using Targeted DNA Enrichment

Egie E. Enabulele, Winka Le Clec'h, Emma K. Roberts, Cody W. Thompson, Molly M. McDonough, Adam W. Ferguson, Robert D. Bradley, Timothy J. C. Anderson, Roy N. Platt II

More than 60 zoonoses are linked to small mammals, including some of the most devastating pathogens in human history. Millions of museum-archived tissues are available to understand natural history of those pathogens. Our goal was to maximize the value of museum collections for pathogen-based research by using targeted sequence capture. We generated a probe panel that includes 39,916 80-bp RNA probes targeting 32 pathogen groups, including bacteria, helminths, fungi, and protozoans. Laboratory-generated, mock-control samples showed that we are capable of enriching targeted loci from pathogen DNA 2,882–6,746-fold. We identified bacterial species in museum-archived samples, including *Bartonella*, a known human zoonosis. These results showed that probe-based enrichment of pathogens is a highly customizable and efficient method for identifying pathogens from museum-archived tissues.

Many serious human pathogens result from zoonotic transmission, including 61% of known human pathogens and 75% of emerging human pathogens (1). For example, rabies virus is transmitted by saliva of infected animals (2). The plague bacteria (*Yersinia pestis*), the causative agent of the largest documented pandemic in human history that reduced the population of Europe by 30%–50%, was transmitted from rats to humans by fleas (3). Other zoonoses include Ebola virus (4), tularemia (*Francisella tularensis*) (5), and tuberculosis (6). The SARS-CoV-2 pandemic, thought to have a bat reservoir, has stimulated renewed emphasis on zoonotic pathogen surveillance (7,8).

Natural history museums are repositories of biologic information in the form of voucher specimens

that represent a major, underused resource for studying zoonotic pathogens (9–13). Originally, specimens were archived as dried skin and skeletal vouchers or preserved in fluids (ethanol) after fixation with formalin or formaldehyde. Now, best practices include preserving specimens and associated soft tissues in liquid nitrogen (–190°C) or mechanical freezers (–80°C) from the time they are collected (14). Those advances in preservation make it possible to extract high-quality DNA and RNA that can be used for pathogen surveillance. For example, retroactive sampling of archived tissues from the US Southwest found that Sin Nombre virus, a New World hantavirus, was circulating in wild rodent populations almost 20 years before the first human cases were reported (15).

It is critical to develop a range of tools for extracting pathogen information from museum-archived samples. Targeted sequencing using probe enrichment has become the tool of choice for medical genomics (16), population genetics (17), phylogenetics (18), and ancient DNA (19,20). Those methods are designed to enrich small amounts of DNA target from a background of contaminating DNA. Probe-based, targeted sequencing has been used to enrich pathogens from complex host–pathogen DNA mixtures (21). For example, Keller et al. used probes to capture and sequence complete *Y. pestis* genomes from burial sites >1,500 years old (22). Enrichment is frequently achieved by designing a panel of probes to specifically target a handful of pathogens of interest (23,24). Similarly, commercial probe sets are available for many types of viruses and human pathogens (23–25). However, many of these probe sets are limited to specific pathogens that might not infect other host species.

Our goal was to develop a panel of biotinylated baits, or probes, to identify the eukaryotic and bacterial pathogens responsible for 32 major zoonoses (Table 1). We aimed to capture both known and related pathogens, using the fact that probes can capture sequences that are ≤10% divergent. To perform this

Author affiliations: Texas Biomedical Research Institute, San Antonio, Texas, USA (E.E. Enabulele, W. Le Clec'h, T.J.C. Anderson, R.N. Platt II); Texas Tech University, Lubbock, Texas, USA (E.K. Roberts, R.D. Bradley); University of Michigan, Ann Arbor, Michigan, USA (C.W. Thompson); Chicago State University, Chicago, Illinois, USA (M.M. McDonough); Field Museum of Natural History, Chicago (A.W. Ferguson)

DOI: <https://doi.org/10.3201/eid2908.221818>

capture, we used a modified version of the ultraconserved element (UCE) targeted sequencing technique (26,27) to specifically enrich pathogen DNA. Biotinylated baits are designed to target conserved genomic regions among diverse groups of pathogens (Figure 1). The baits are hybridized to a library potentially containing pathogen DNA. Bait-bound DNA fragments are enriched during a magnetic bead purification step before sequencing (Figure 2). The final library contains hundreds or thousands of orthologous loci with single-nucleotide variants or indels from the targeted pathogen groups that can then be used for population or phylogenetic analyses.

## Methods

We have compiled a detailed description of the methods used (Appendix 1, <https://wwwnc.cdc.gov/EID/article/29/8/22-1818-App1.pdf>; <https://doi.org/10.17504/protocols.io.5jyl8jnzrg2w/v1>). Code is available on GitHub ([https://www.github.com/nealplatt/pathogen\\_probes](https://www.github.com/nealplatt/pathogen_probes); <https://doi.org/10.5281/zenodo.7319915>). Raw sequence data are available from the National Center for Biotechnology Information (BioProject PRJNA901509; Appendix 2, <https://wwwnc.cdc.gov/EID/article/29/8/22-1818-App2.xlsx>). A summary of our methods follows.

[wwwnc.cdc.gov/EID/article/29/8/22-1818-App2.xlsx](https://wwwnc.cdc.gov/EID/article/29/8/22-1818-App2.xlsx)). A summary of our methods follows.

## Panel Development

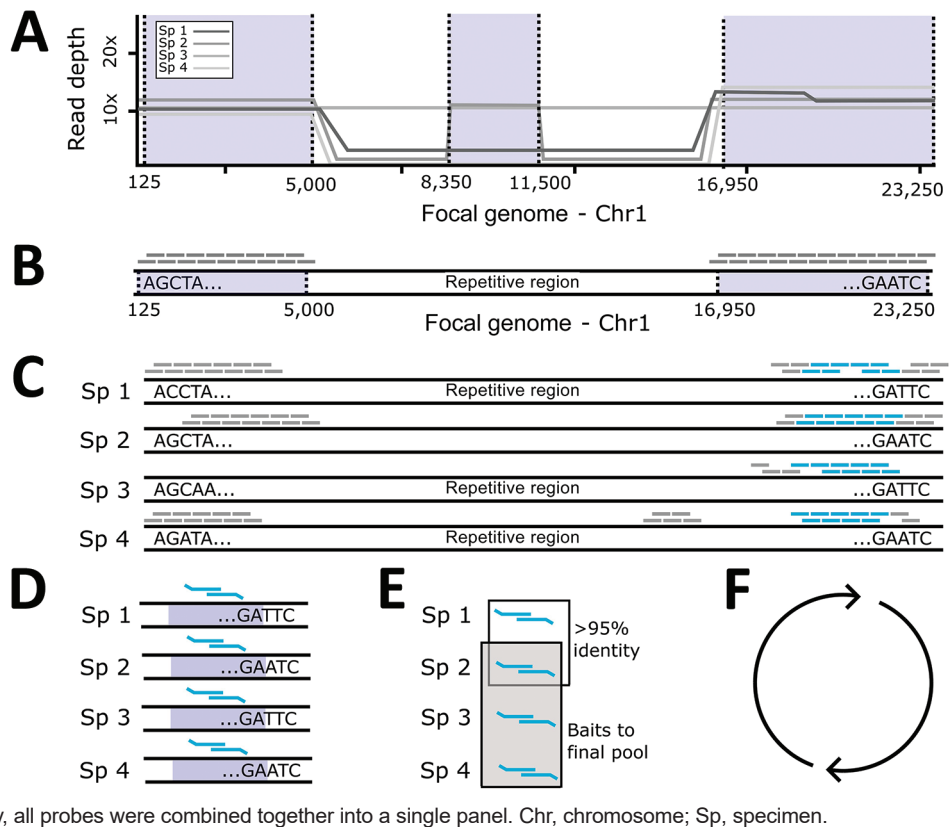
We developed a panel of baits for targeted sequencing of 32 zoonotic pathogens. To develop this panel, we used the Phyluce version 1.7.1 (26,27) protocol to design baits for conserved loci within each pathogen group. First, we simulated and mapped reads from each species within a pathogen group to a focal genome assembly (Table 1; Figure 1, panel A). We used the mapped reads to identify putative orthologous loci that were >80% similar across the group and generated in silico baits from the focal genome (Figure 1, panel B). These baits were mapped back to each member (Figure 1, panel C) to identify single-copy orthologs within the group. Next, we designed 2 overlapping 80-bp baits from loci in each member of the group (Figure 1, panel D) and removed baits with >95% sequence similarity (Figure 1, panel E). We repeated those steps for each pathogen group (Figure 1, panel F). We compared the remaining baits with mammalian genomes and replaced them to minimize

**Table 1.** Zoonotic pathogens targeted for DNA enrichment in study of prospecting for zoonotic pathogens by using targeted DNA enrichment

Pathogen group	Taxonomic level	Focal pathogen	Zoonoses
<i>Anaplasma</i>	Genus	<i>Anaplasma phagocytophilum</i>	Anaplasmosis
Apicomplexa	Phylum	<i>Plasmodium falciparum</i>	Malaria
<i>Bacillus cereus</i> group*	Species group	<i>Bacillus anthracis</i>	Anthrax
<i>Bartonella</i>	Genus	<i>Bartonella bacilliformis</i>	Cat-scratch fever
<i>Borrelia</i>	Genus	<i>Borrelia burgdorferi</i>	Lyme disease
<i>Burkholderia</i>	Genus	<i>Burkholderia mallei</i>	Glanders
<i>Campylobacter</i>	Genus	<i>Campylobacter jejuni</i>	Campylobacteriosis
Cestoda	Class	<i>Taenia multiceps</i>	Taeniasis
<i>Chlamydia</i>	Genus	<i>Chlamydia trachomatis</i>	Chlamydia
<i>Coxiella</i>	Genus	<i>Coxiella burnetii</i>	Q fever
<i>Ehrlichia</i>	Genus	<i>Ehrlichia canis</i>	Ehrlichiosis
Eurotiales	Order	<i>Talaromyces marneffeii</i>	Talaromycosis
<i>Francisella</i>	Genus	<i>Francisella tularensis</i>	Tularemia
Hexamitidae	Family	<i>Giardia intestinalis</i>	Giardiasis
Kinetoplastea	Class	<i>Leishmania major</i>	Leishmaniasis
<i>Leptospira</i>	Genus	<i>Leptospira interrogans</i>	Leptospirosis
<i>Listeria</i>	Genus	<i>Listeria monocytogenes</i>	Listeriaosis
<i>Mycobacterium</i>	Genus	<i>Mycobacterium tuberculosis</i>	Tuberculosis
Nematodes (clade I)	Phylum (clade)	<i>Trichinella spiralis</i>	Trichinosis
Nematodes (clade III)	Phylum (clade)	<i>Brugia malayi</i>	Filariasis
Nematodes (clade IVa)	Phylum (clade)	<i>Strongyloides stercoralis</i>	Strongyloidiasis
Nematodes (clade IVb)	Phylum (clade)	<i>Steinernema carpocapsae</i>	None
Nematodes (clade V)	Phylum (clade)	<i>Haemonchus contortus</i>	None
Onygenales	Order	<i>Histoplasma capsulatum</i>	Histoplasmosis
<i>Pasteurella</i>	Genus	<i>Pasteurella multocida</i>	Pasteurellosis
<i>Rickettsia</i>	Genus	<i>Rickettsia rickettsii</i>	Typhus
<i>Salmonella</i>	Genus	<i>Salmonella enterica</i>	Salmonellosis
<i>Streptobacillus</i>	Genus	<i>Streptobacillus moniliformis</i>	Rat-bite fever
Trematoda	Class	<i>Schistosoma mansoni</i>	Schistosomiasis
Tremellales	Order	<i>Cryptococcus neoformans</i>	Cryptococcosis
<i>Trypanosoma</i> *	Genus	<i>Trypanosoma cruzi</i>	Sleeping sickness
<i>Yersinia</i>	Genus	<i>Yersinia pestis</i>	Plague

\*Supplemented with additional probes/baits.

**Figure 1.** Probe panel design for study of prospecting for zoonotic pathogens by using targeted DNA enrichment. A) Simulated reads from each pathogen within a group were mapped back to a single focal genome. B) We identified regions with consistent coverage from each member of the pathogen group to identify putative, orthologous loci and generated a set of *in silico* probes from the focal genome. C) Those *in silico* probes were then mapped back to the genomes of each member in the pathogen group to find single copy, orthologous regions, present in most members. D, E) We designed 2 overlapping 80-bp baits to target the loci in each member of the pathogen group (D) and compared them with each another to remove highly similar probes (E). One probe was retained from each group of probes with high sequence similarity (>95%). F) We identified the probes necessary to capture 49 loci in that pathogen group. This process was repeated for the next pathogen group. Finally, all probes were combined together into a single panel. Chr, chromosome; Sp, specimen.

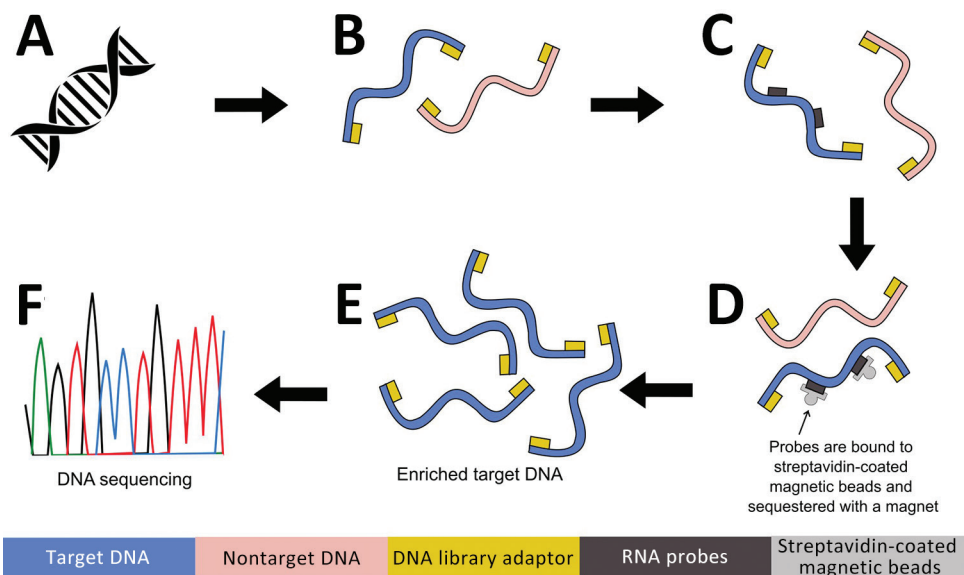


cross-reactivity with the host. Finally, we combined baits to capture 49 loci from each pathogen group into a panel that was synthesized by Daicel Arbor Biosciences (<https://arborbiosci.com>).

**Museum-Archived and Control Samples**

We extracted DNA from 38 museum samples by using the DNeasy Kit (QIAGEN, <https://www.qiagen.com>) (Table 2). We generated control samples

**Figure 2.** Targeted DNA enrichment workflow for study of prospecting for zoonotic pathogens by using targeted DNA enrichment. A) Genomic DNA extracted using the DNeasy Kit (QIAGEN, <https://www.qiagen.com>). B) Next-generation sequencing libraries prepared using KAPA Hyperplus Kit (<https://www.biocompare.com>) and barcoding each library with IDT xGen Stubby Adaptor-UDI Primers (<https://www.idtdna.com>). C) RNA probes hybridization using the high sensitivity protocol of myBaits version 5. (<https://arborbiosci.com>). D) Probes bound to streptavidin-coated magnetic beads and sequestered with a magnet (E) 15 cycles PCR amplification of enriched libraries. F) Libraries sequenced on an Illumina Hi-Seq 2500 platform (<https://www.illumina.com>).



by spiking naive mouse DNA with 1% microorganism DNA from *Mycobacterium bovis*, *M. tuberculosis*, *Plasmodium vivax*, *P. falciparum*, and *Schistosoma mansoni*. We then further diluted an aliquot of this 1% pathogen mixture into mouse DNA to create a 0.001% host–pathogen mixture. This range was designed to test the lower limits of detection but also represent a reasonable host–pathogen proportion.

For example, *Theileria parva*, a tick-transmitted apicomplexan, is present in samples from 0.9% through 3% (28), and 1.5% of DNA sequence reads in clinical blood samples is from *P. vivax* (29).

### Library Preparation

We generated standard DNA sequencing libraries from 500 ng of DNA per sample. We combined

**Table 2.** Specimens examined using targeted sequencing in study of prospecting for zoonotic pathogens by using targeted DNA enrichment\*

Museum accession no.	Source species (common name)	Locality, country: state, county	Date	SRA ID
TK48533	<i>Myotis volans</i> (long-legged myotis)	Mexico: Durango, Arroyo El Triguero	1995 May 18	SAMN31718202
TK49668	<i>Didelphis virginiana</i> (Virginia opossum)	United States: Texas, Kerr	1996 May 14	SAMN31718203
TK49674	<i>Peromyscus attwateri</i> (Texas mouse)	United States: Texas, Kerr	1996 May 14	SAMN31718204
TK49686	<i>Peromyscus laceianus</i> (deer mouse)	United States: Texas, Kerr	1996 May 14	SAMN31718205
TK49712	<i>Dasyurus novemcinctus</i> (nine-banded armadillo)	United States: Texas, Kerr	1996 May 16	SAMN31718206
TK49732	<i>Lasiurus borealis</i> (eastern red bat)	United States: Texas, Kerr	1996 May 17	SAMN31718207
TK49733	<i>Myotis velifer</i> (vesper bat)	United States: Texas, Kerr	1996 May 16	SAMN31718208
TK57832	<i>P. attwateri</i>	United States: Texas, Kerr	1997 May 14	SAMN31718209
TK70836	<i>Desmodus rotundus</i> (common vampire bat)	Mexico: Durango, San Juan de Camarones	1997 Jun 27	SAMN31718210
TK90542	<i>Sigmodon hirsutus</i> (southern cotton rat)	Mexico: Chiapas, Comitán	1999 Jul 9	SAMN31718211
TK93223	<i>Peromyscus melanophrys</i> (plateau mouse)	Mexico: Oaxaca, Las Minas	2000 Jul 13	SAMN31718212
TK93289	<i>Carollia subrufa</i> (gray short-tailed bat)	Mexico: Chiapas, Ocozocoautla	2000 Jul 16	SAMN31718213
TK93402	<i>Chaetodipus eremicus</i> (Chihuahan pocket mouse)	Mexico: Coahuila	2000 Jul 22	SAMN31718214
TK101275	<i>Glossophaga commissarisi</i> (Commissaris' long-tongued bat)	Honduras: Comayagua, Playitas	2001 Jul 10	SAMN31718215
TK136205	<i>Heteromys desmarestianus</i> (Desmarest's spiny pocket mouse)	Honduras: Atlantida, Jardin Botanico Lancetilla	2004 Jul 16	SAMN31718216
TK136222	<i>Peromyscus mexicanus</i> (Mexican deer mouse)	Honduras: Colon, Trujillo	2004 Jul 17	SAMN31718217
TK136228	<i>H. desmarestianus</i>	Honduras: Colon, Trujillo	2004 Jul 17	SAMN31718218
TK136240	<i>Glossophaga soricine</i> (Pallas's long-tongued bat)	Honduras: Colon, Trujillo	2004 Jul 16	SAMN31718219
TK136756	<i>Eptesicus furinalis</i> (Argentine brown bat)	Honduras: Colon, Trujillo	2004 Jul 17	SAMN31718220
TK136783	<i>Glossophaga leachii</i> (gray long-tongued bat)	Honduras: Colon, Trujillo	2004 Jul 17	SAMN31718221
TK148935	<i>Rhogeessa tumida</i> (back-winged little yellow bat)	Mexico: Tamaulipas, Soto la Marina	2008 Jul 27	SAMN31718222
TK148943	<i>M. velifer</i>	Mexico: Tamaulipas, Soto la Marina	2008 Jul 27	SAMN31718223
TK150290	<i>Balantiopteryx plicata</i> (gray sac-winged bat)	Mexico: Michoacan, El Marqués	2006 Jul 22	SAMN31718224
TK154677	<i>Gerbilliscus leucogaster</i> (bushveld gerbil)	Botswana: Ngamiland, Koanaka Hills	2008 Jun 29	SAMN31718225
TK154685	<i>G. leucogaster</i>	Botswana: Ngamiland, Koanaka Hills	2008 Jun 29	SAMN31718226
TK154687	<i>G. leucogaster</i>	Botswana: Ngamiland, Koanaka Hills	2008 Jun 29	SAMN31718227
TK164683	<i>Mastomys natalensis</i> (Natal multimammate mouse)	Botswana: Ngamiland, Koanaka Hills	2009 Jul 18	SAMN31718228
TK164686	<i>M. natalensis</i>	Botswana: Ngamiland, Koanaka Hills	2009 Jul 18	SAMN31718229
TK164689	<i>M. natalensis</i>	Botswana: Ngamiland, Koanaka Hills	2009 Jul 18	SAMN31718230
TK164690	<i>M. natalensis</i>	Botswana: Ngamiland, Koanaka Hills	2009 Jul 18	SAMN31718231
TK164702	<i>M. natalensis</i>	Botswana: Ngamiland, Koanaka Hills	2009 Jul 19	SAMN31718232
TK164714	<i>M. natalensis</i>	Botswana: Ngamiland, Koanaka Hills	2009 Jul 19	SAMN31718233
TK164728	<i>M. natalensis</i>	Botswana: Ngamiland, Koanaka Hills	2009 Jul 19	SAMN31718234
TK166246	<i>P. attwateri</i>	United States: Texas, Kerr	2010 May 17	SAMN31718235
TK179690	<i>P. attwateri</i>	United States: Texas, Kerr	2013 May 20	SAMN31718236
TK185677	<i>P. attwateri</i>	United States: Texas, Kerr	2018 May 21	SAMN31718237
TK197046	<i>P. attwateri</i>	United States: Texas, Kerr	2016 May 26	SAMN31718238
TK199855	<i>P. attwateri</i>	United States: Texas, Kerr	2019 May 21	SAMN31718239

\*ID, identification; SRA, National Center for Biotechnology Information Sequence Read Archive.

individual libraries with similar DNA concentrations into pools of 4 samples and used the myBaits version 5 (Daicel Arbor Biosciences) high sensitivity protocol to enrich target loci. We used 2 rounds of enrichment (24 h at 65°C), washed away unbound DNA, and amplified the remainder for 15 cycles before pooling for sequencing.

### Classifying Reads

First, we generated a dataset of target loci by mapping the probes to representative and reference genomes in RefSeq v212 with BMap v38.96 (30). For each probe, we kept the 10 best sites that mapped with  $\geq 85\%$  sequence identity along with 1,000 bp upstream and downstream. These sequences were combined into a database to classify reads by using Kraken2 version 2.1.1 (31) (Figure 3, panel A). Next, we extracted pathogen reads with KrakenTools version 1.2 (<https://github.com/jenniferlu717/KrakenTools>). We assembled those reads (Figure 3, panel B) with the SPAdes genome assembler version 3.14.1 (32) and filtered them to remove low quality contigs (<100 bp and <10 $\times$  median coverage). We removed samples that had <2 contigs from downstream analyses. During this time, we extracted target loci in available reference genomes (Figure 3, panel C). Next, we identified (Figure 3, panel D), aligned and trimmed (Figure 3, panel E) orthologs before concatenating them into a single alignment (Figure 3, panel F). Finally, we

generated and bootstrapped a phylogenetic tree (Figure 3, panel G) by using RaxML-NG version 1.0.1 (33). We repeated those steps for each pathogen group (Figure 3, panel H).

### Host Identification

There were sufficient mtDNA sequences from most samples to verify museum identifications by comparing reads to a Kraken2 version 2.1.2 (31) database of mammalian mitochondrial genomes. We filtered the classifications by removing samples with <50 classified reads and single-read, generic classifications.

## Results

### Panel Development

We used the ultraconserved element protocol developed by Faircloth et al. (26,27) to develop a set of 39,893 biotinylated baits that target 32 pathogen groups responsible for 32 zoonoses. Each pathogen group is targeted at 49 loci with a few diverse taxa, *Bacillus cereus* and *Trypanosoma* species, targeted at 98 loci. We compiled information on pathogen groups, focal taxa, genome accessions, and number of baits (Table 3).

### Control Samples

We tested the efficacy of our bait set on laboratory-made host–pathogen mixtures containing DNA from

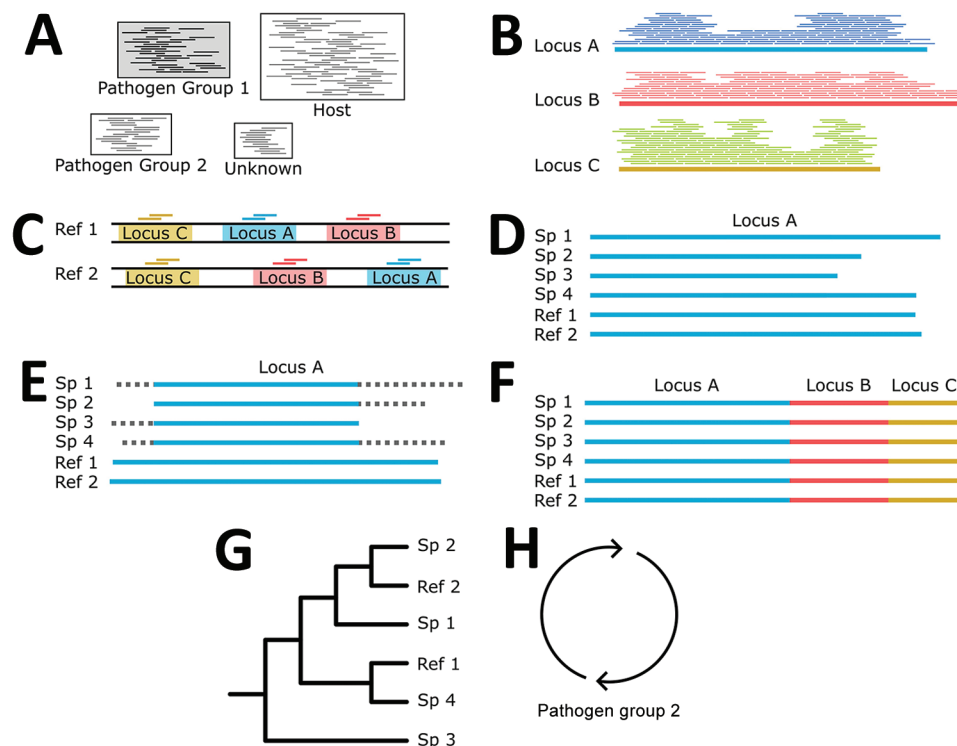


**Figure 3.** Building phylogenies from parasite reads for study of prospecting for zoonotic pathogens by using targeted DNA enrichment. A) After read classification, we extracted all the reads associated with a pathogen group. B) Those reads were assembled into contigs with a genome assembler. C) Simultaneously, we identified and extracted the target loci from all members of the pathogen group with available reference genomes to ensure that our final phylogeny has representatives from as many members of the pathogen group as possible. D, E) For each targeted locus, we combined the assembled contigs (D) and genome extracted loci for (E) multiple sequence alignment and trimming. F, G) Each aligned and trimmed locus is concatenated together (F) for phylogenetic analyses (G). H) If necessary, those steps are repeated for reads classified in other pathogen groups. Ref, reference; Sp, specimen.

**Table 3.** Summary of probes developed for targeted capture of pathogen DNA in study of prospecting for zoonotic pathogens by using targeted DNA enrichment

Pathogen group	Type	Probe count	Locus count	RefSeq genome count	Focal pathogen	GenBank accession no.
<i>Anaplasma</i>	Bacteria	368	49	57	<i>Anaplasma phagocytophilum</i>	GCF000013125
Apicomplexa	Eukaryote	3,219	49	64	<i>Plasmodium falciparum</i>	GCA000002765
<i>Bacillus cereus</i> group*	Bacteria	833	98	134	<i>Bacillus anthracis</i>	GCF000008165
<i>Bartonella</i>	Bacteria	1,812	49	31	<i>Bartonella bacilliformis</i>	GCF000015445
<i>Borrelia</i>	Bacteria	688	49	16	<i>Borrelia burgdorferi</i>	GCF000502155
<i>Burkholderia</i>	Bacteria	683	49	39	<i>Burkholderia mallei</i>	GCF000011705
<i>Campylobacter</i>	Bacteria	2,194	49	33	<i>Campylobacter jejuni</i>	GCF000009085
Cestoda	Eukaryote	907	49	18	<i>Taenia multiceps</i>	GCA001923025
<i>Chlamydia</i>	Bacteria	830	49	15	<i>Chlamydia trachomatis</i>	GCF000008725
<i>Coxiella</i>	Bacteria	144	49	70	<i>Coxiella burnetii</i>	GCF000007765
<i>Ehrlichia</i>	Bacteria	235	49	7	<i>Ehrlichia canis</i>	GCF000012565
Eurotiales	Eukaryote	4,097	49	158	<i>Talaromyces marneffeii</i>	GCF000001985
<i>Francisella</i>	Bacteria	470	49	14	<i>Francisella tularensis</i>	GCF000008985
Hexamitidae	Eukaryote	782	49	19	<i>Giardia intestinalis</i>	GCA000002435
Kinetoplastea	Eukaryote	2,917	49	49	<i>Leishmania major</i>	GCF000002725
<i>Leptospira</i>	Bacteria	2,517	49	69	<i>Leptospira interrogans</i>	GCF000009255
<i>Listeria</i>	Bacteria	765	49	23	<i>Listeria monocytogenes</i>	GCF000196035
<i>Mycobacterium</i>	Bacteria	2,463	49	86	<i>Mycobacterium tuberculosis</i>	GCF000195955
Nematodes, clade I	Eukaryote	357	49	13	<i>Trichinella spiralis</i>	GCA000181795
Nematodes, clade III	Eukaryote	1,494	49	25	<i>Brugia malayi</i>	GCA000002995
Nematodes, clade IVa	Eukaryote	252	49	7	<i>Strongyloides stercoralis</i>	GCA000947215
Nematodes, clade IVb	Eukaryote	1,487	43	34	<i>Steinernema carpocapsae</i>	GCA0000757645
Nematodes, clade V	Eukaryote	3,242	48	47	<i>Haemonchus contortus</i>	GCA007637855
Onygenales	Eukaryote	1,973	49	38	<i>Histoplasma capsulatum</i>	GCF000149585
<i>Pasteurella</i>	Bacteria	615	49	11	<i>Pasteurella multocida</i>	GCF000754275
<i>Rickettsia</i>	Bacteria	394	49	37	<i>Rickettsia rickettsii</i>	GCF001951015
<i>Salmonella</i>	Bacteria	145	49	35	<i>Salmonella enterica</i>	GCF001159405
<i>Streptobacillus</i>	Bacteria	245	49	7	<i>Streptobacillus moniliformis</i>	GCF000024565
Trematoda	Eukaryote	924	49	18	<i>Schistosoma mansoni</i>	GCA000237925
Tremellales	Eukaryote	1,999	49	26	<i>Cryptococcus neoformans</i>	GCF000091045
Trypanosoma*	Eukaryote	617	97	10	<i>Trypanosoma cruzi</i>	GCF000209065
<i>Yersinia</i>	Bacteria	225	49	22	<i>Yersinia pestis</i>	GCF000009065

\*Supplemented.

*Mus musculus*, *Mycobacterium tuberculosis*, *Plasmodium falciparum*, *P. vivax*, and *Schistosoma mansoni*. We generated 4 control samples containing either 1% or 0.001% pathogen DNA that was enriched or not enriched. We classified reads against the database of target loci and found that 42.7% of all reads (*Mycobacterium* = 13.1%, *Plasmodium* = 28.1%, *Schistosoma* = 1.5%) were from control pathogens in the 1% enriched control sample. However, only 0.03% of the corresponding 1% unenriched control was from target loci. Aside from the raw percentages, we compared the coverage of each probed region in the 1% enriched and unenriched control samples (Figure 4, panels B–D) to understand how enrichment effected coverage at each locus. Mean coverage per *Mycobacterium* locus increased from 0.14× to 944.5× (6,746-fold enrichment), 0.53× to 1,527.4× for *Plasmodium* loci (2,882-fold enrichment), and 0.02× to 117.9× (5,895-fold enrichment) for schistosome loci. Because the sequencing library from the 0.001% unenriched sample did not work during the sequencing reaction, we do not have a baseline to examine enrichment in the 0.001% samples.

We extracted reads assigned to each pathogen group and assembled and aligned them with target loci extracted from reference genomes of closely related species by using tools from PhyLuce version 1.7.1 (26,27). We were able to assemble 0–23 target loci per pathogen group in the control samples (Table 4). Assembled loci varied in size from 109 to 1,991 bp (median 636.5 bp). For each sample/group with >2 loci captured, we generated a phylogenetic tree along with other members of the taxonomic group (Figure 5). In each case, pathogen loci from the control samples were sister groups to the appropriate reference genome with strong bootstrap support. For example, the *Schistosoma* loci assembled from the 1% enriched control sample were sister to the *S. mansoni* genome (GCA000237925) in 100% of bootstrap replicates.

### Museum Samples

Next, we tested our bait set on museum-archived tissues. We generated 649.3 million reads across all 38 samples (mean 17.1 million reads/sample). An initial classification showed that, on average, 4.3% of reads



**Table 4.** Parasite reads identified in and loci assembled from control samples

Enriched	Pathogen concentration, %	Total reads	<i>Schistosoma</i>		<i>Plasmodium</i>		<i>Mycobacterium</i>	
			Reads	Loci	Reads	Loci	Reads	Loci
True	0.001	509,672	3	0	168	7	556	0
True	1	398,469	5,879	23	52,274	8	112,141	23
False	1	375,786	15	0	17	0	83	0

such that 18 samples had <12 reads and 18 samples had >1,000 reads (median 552 reads/sample). In 5 samples, the percentage of *Bartonella* reads was exceedingly high (>10%). In comparison, the median number of *Plasmodium* reads never exceeded 0.04% of reads from a single museum sample (mean 158.5 reads/sample).

We used phylogenetic analyses and rules of monophyly to identify putative pathogens to species or strain for each of the 15 genera with  $\geq 1,000$  reads (Figure 4, panel A). We were unable to assemble >1 target locus for any specimen in 13 genera. We were able to assemble 3–20 loci (mean 8 loci/sample) from 16 samples containing *Bartonella* (Figure 6), 3 loci from a sample containing *Paraburkholderia* reads (Figure 7), and 8 loci from a sample containing *Ralstonia* reads (Figure 8).

### Host Identification

We compared reads from each sample to a database of mitochondrial genomes to identify the host. In gen-

eral, reads from the mitochondria comprised a small proportion ( $\leq 1\%$ , mean 0.04%) of each sample (Figure 9). Despite the low number of mitochondrial reads, generic classifications from the mitochondrial database coincided with the museum identifications after filtering samples with  $\leq 50$  mitochondrial reads. For the remaining samples, the correct genus was identified by >85% (mean 98%) of reads from that sample. Classifying reads less than the generic level is limited by mitochondrial genome availability, but where possible, we were able to confirm museum identifications at the species level.

### Discussion

We developed a set of 39,893 biotinylated baits for targeted sequencing of >32 zoonotic pathogens, and their relatives, from host DNA samples. To test the efficacy of the bait panel, we used 4 control samples that contained either 1% or 0.001% pathogen DNA and further subdivided into pools that were enriched and unenriched. Our results (Figure 4) showed a

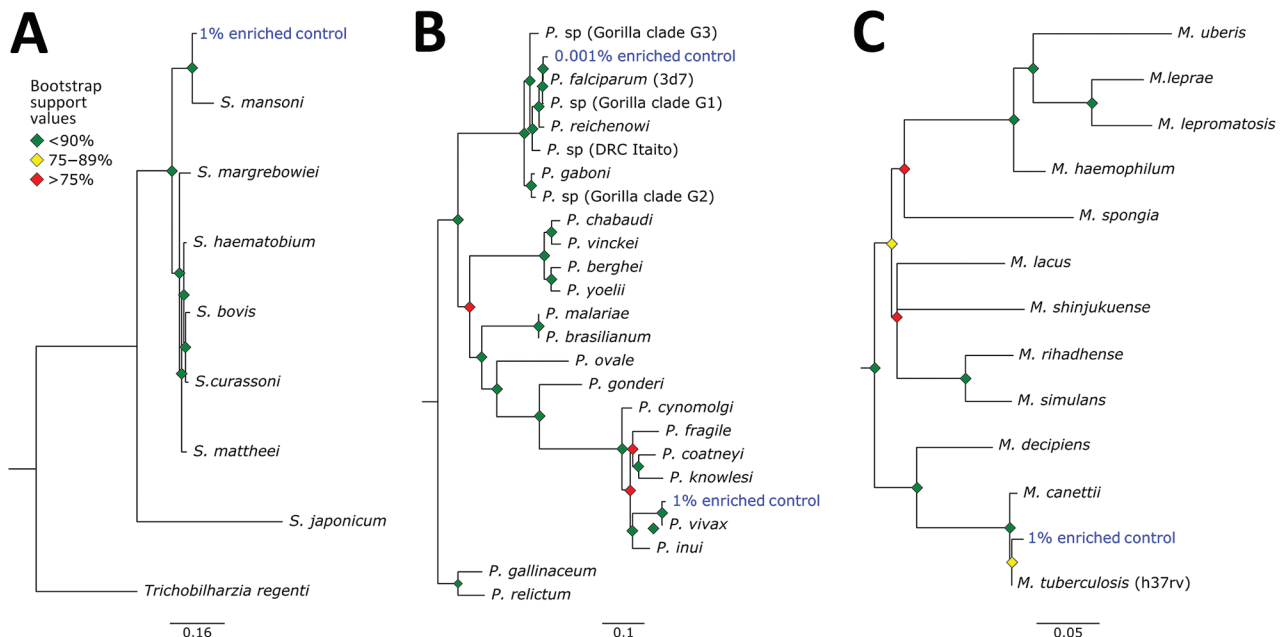


**Figure 5.** Phylogenetic analysis of pathogens used in control samples for study of prospecting for zoonotic pathogens by using targeted DNA enrichment. A) *Schistosoma*; B) *Plasmodium*; C) *Mycobacterium*. Reads from each control pathogen (*M. tuberculosis*, *P. falciparum*, *P. vivax*, and *S. mansoni*) were extracted, assembled, aligned, and trimmed for maximum-likelihood phylogenetic analyses. The phylogenies were used to identify the species or strain of pathogen used in the controls. Blue indicates control samples. Bootstrap support values are indicated by colored diamonds at each available node. Branches with <50% bootstrap support were collapsed. Nodal support is indicated by color coded diamonds. Scale bars indicate nucleotide substitutions per site. Assembly accession numbers (e.g., GCA902374465) and tree files are available from <https://doi.org/10.5281/zenodo.8014941>.



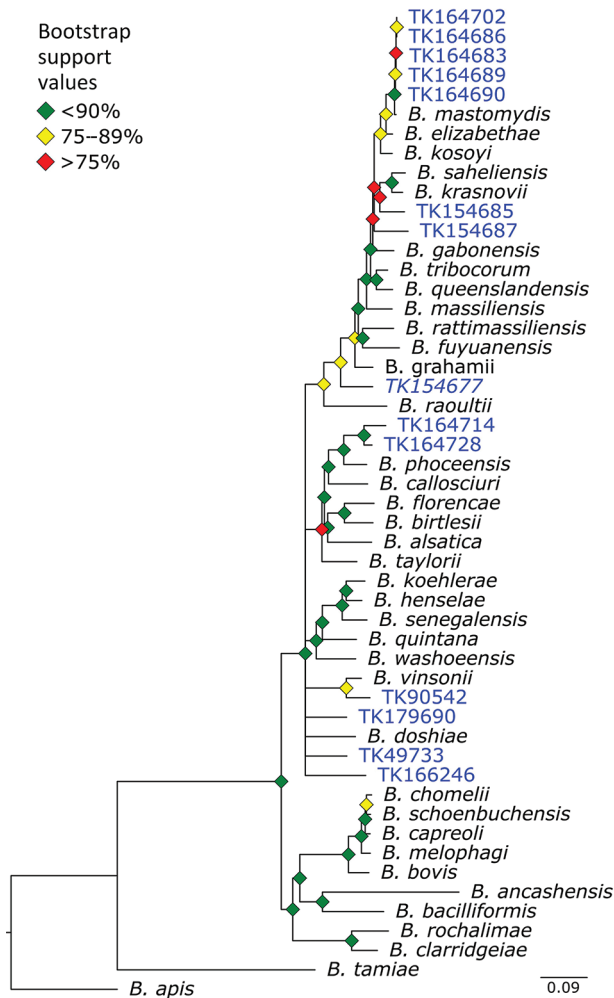


**Figure 6.** Phylogenetic analysis of *Bartonella* using museum archived samples in study of prospecting for zoonotic pathogens by using targeted DNA enrichment. Blue indicates museum archived samples; museum accession numbers are given (Table 1). Branches with <50% bootstrap support were collapsed. Nodal support is indicated by color coded diamonds. Scale bar indicates nucleotide substitutions per site. Assembly accession numbers (e.g., CA902374465) and tree files are available from <https://doi.org/10.5281/zenodo.8014941>.

large increase of pathogen DNA in the 1% enriched sample when compared with its unenriched counterpart. Specifically, enrichment increased the amount of pathogen DNA from 0.03% to 42.1%.

We were able to generate phylogenetically informative loci from *Plasmodium*, *Mycobacterium*, and *Schistosoma* species in the 1% enriched control sample. On the basis of genome size, we estimate genome copies as 91,611 for *Plasmodium*, 261,030 for *Mycobacterium*, and 3,159 for *Schistosoma* in the control sample. This finding indicates that the probe set is able to detect these pathogens from even a few thousand

genome copies per sample (*Schistosoma* species). In contrast, we were only able to generate phylogenetically informative loci from *P. falciparum* in 0.001% enriched sample, which would hypothetically contain  $\approx 39$  genome copies. This finding implies that the bait set might be capable of identifying pathogens present in samples with only a few hundred genome copies. However, there are limitations to *Plasmodium* detection that should be considered.

In each sample, reads were detected from only a few loci rather than from the entire genome. For example, in the 1% enriched sample, 5,879 of the 398,469 reads came from 32 loci totaling 19.6 kb. Had the unenriched sample contained the same number of reads, randomly distributed across the genome, it would have amounted to 1 read every 62 kb. We found that enrichment increased coverage at probed loci from 0.23 $\times$  to 863.3 $\times$ , a 3,732.3-fold increase when averaged across all pathogens/loci (Figure 4). Those results show that although large amounts of host DNA might remain in a sample, the targeted loci are greatly enriched.

We tested the panel of baits on 38, museum-archived, small mammal samples without previous knowledge of infection history. Reads from these samples were initially designated to 93 different genera, but most of these genera contained a limited number of reads. For example, almost half of the 93 genera ( $n = 43$ ) were identified on the basis of a single read across all 38 samples, most likely a bioinformatic artifact. We identified 15 genera in which 1 sample had  $\geq 1,000$  reads. For each of these 15 genera, we extracted any reads classified within the same family (e.g., genus *Bartonella*, family Bartonellaceae) and assembled, aligned, and trimmed them for phylogenetic analyses. In most cases, the reads failed the assembly step ( $n = 6$ ), were filtered on the basis of locus size or coverage ( $n = 5$ ), or assembled into multiple loci that were not targeted by our bait set ( $n = 2$ ); we did not pursue those reads any further. However, we were able to generate phylogenies for specimens positive for *Bartonella*, *Ralstonia*, and *Paraburkholderia* species.

*Bartonella* is a bacterial genus responsible for cat-scratch disease, Carrión's disease, and trench fever (34). Transmission often occurs between humans and their pets or from infected fleas ticks, or other arthropod vectors (35). We were able to recover target loci for 14 of 36 specimens. A phylogeny of *Bartonella* species placed the museum samples in multiple clades (Figure 6). For example, 5 specimens formed a monophyletic clade sister to *B. mastomydis*. *B. mastomydis* recently was described from *Mastomys erythroleucus* mice collected in Senegal (36). Appropriately, the

samples we tested were collected from *M. natalensis* mice from Botswana (Table 2). Another clade contained *B. vinsonii* and a *Sigmodon* rat (TK90542) collected in Mexico. Zoonotic transmission of *B. vinsonii* has been implicated in neurologic disorders (37). Other museum samples probably contain novel *Bartonella* species/strains or at least represent species/strains without genomic references.

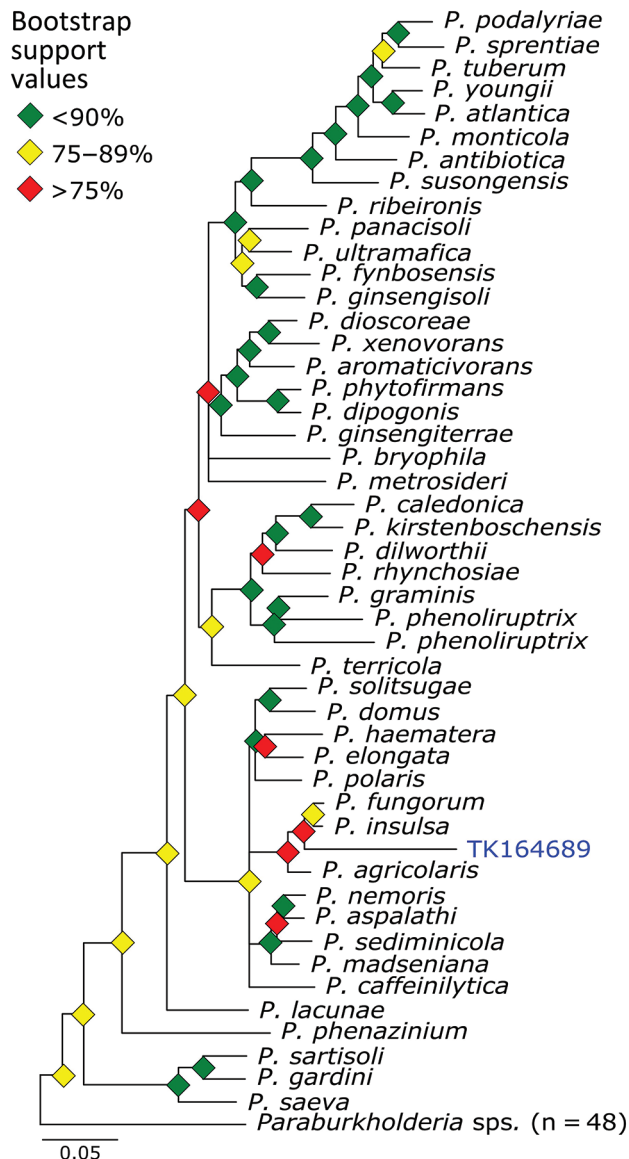


**Figure 7.** Phylogenetic analysis of *Paraburkholderia* using museum archived samples in study of prospecting for zoonotic pathogens by using targeted DNA enrichment. Blue indicates museum archived samples; museum accession numbers are given (Table 1). Branches with <50% bootstrap support were collapsed. Nodal support is indicated by color coded diamonds. Scale bar indicates nucleotide substitutions per site. Assembly accession numbers (e.g., GCA90237446) and tree files are available from <https://doi.org/10.5281/zenodo.8014941>.

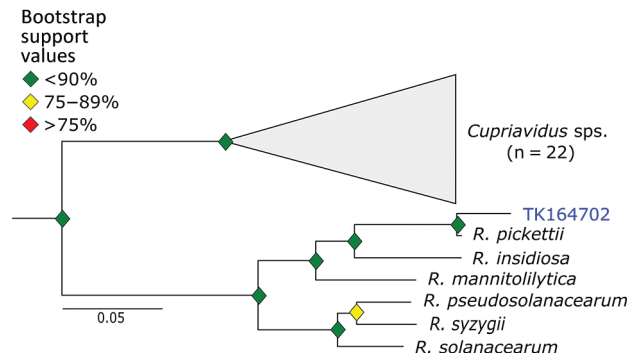


**Figure 8.** Phylogenetic analysis of *Ralstonia* using museum archived samples in study of prospecting for zoonotic pathogens by using targeted DNA enrichment. Blue indicates museum archived samples; museum accession numbers are given (Table 1). Branches with <50% bootstrap support were collapsed. Nodal support is indicated by color coded diamonds. Scale bar indicates nucleotide substitutions per site. Assembly accession numbers (e.g., GCA90237446) and tree files are available from <https://doi.org/10.5281/zenodo.8014941>.

*Paraburkholderia* is a genus of bacteria commonly associated with soil microbiomes and plant tissues. We identified *Paraburkholderia* reads in 3 specimens and were able to place 1 of those in a phylogeny sister to a clade containing *P. fungorum* and *P. insulsa*. Because bootstrap values across the phylogeny were moderate in general, and weak in this particular region (Figure 7), placement of this sample is tenuous. *P. fungorum* is the sole member of *Paraburkholderia* believed to be capable of infecting humans, but it is only a rare, opportunistic, human pathogen (38–40).

*Ralstonia* is a bacteria genus closely related to the genus *Pseudomonas*. We identified *Ralstonia* reads in 5 samples and were able to place a specimen on a phylogeny. This sample is closely affiliated with *R. pickettii* (Figure 8). We are unaware of any examples of zoonotic transmission of *R. pickettii*. Rather, *R. pickettii* has been identified as a common contaminant in laboratory reagents (41), and outbreaks have been caused by contaminated medical supplies (42). We failed to identify nucleic acids in any of our negative controls during library preparation. Furthermore, if there were systemic contamination, we would expect to find *Ralstonia* species in all of our samples, rather than the 5 of 36 observed. Thus, because we cannot rule out reagent contamination, the presence of *Ralstonia* species in the museum samples should be interpreted with caution.

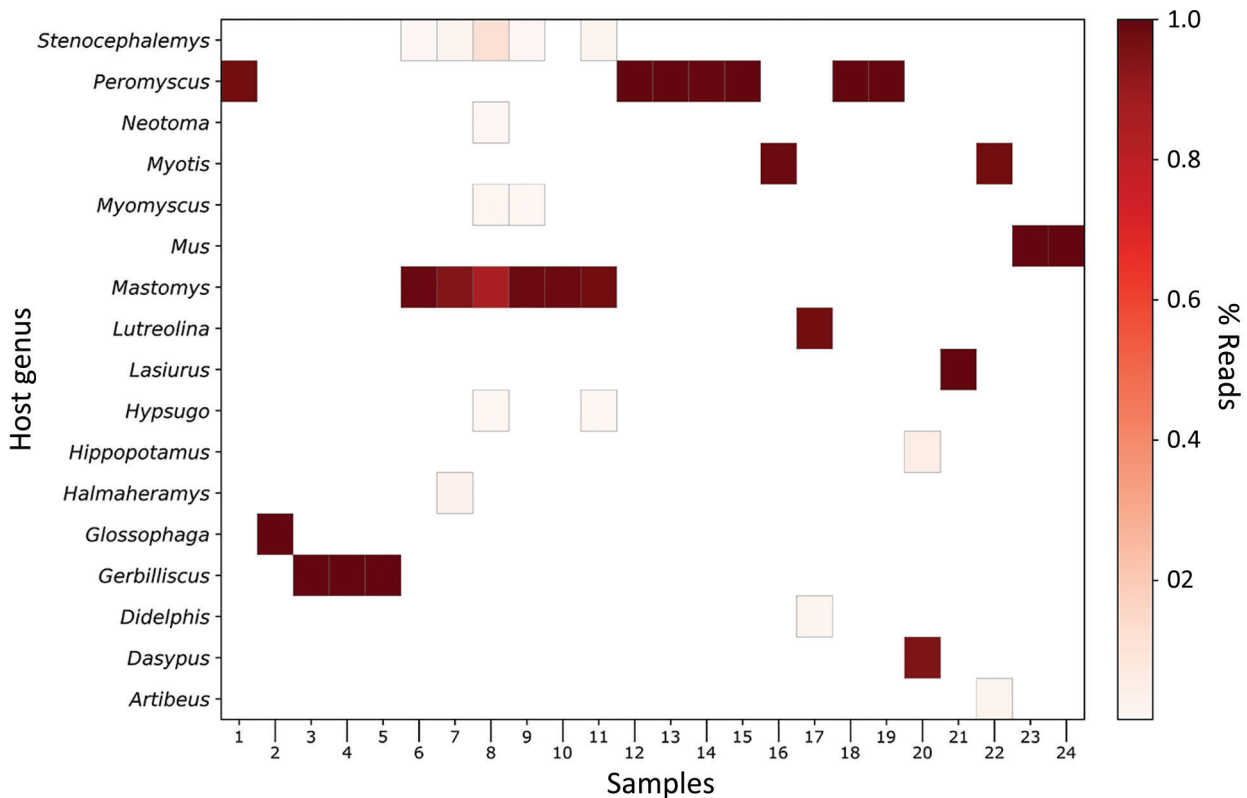
We were able to capture, sequence, and assemble loci from taxa that were not represented in the databases used to design the bait panel. This ability was possible for 2 reasons. First, the bait panel is highly redundant. The baits are sticky and able to capture

nucleic acid fragments that are  $\leq 10\%$ – $12\%$  divergent (43). We designed the panel with  $\leq 5\%$  sequence divergence between any pair of baits at a particular locus (Figure 10). Second, sampled loci within each pathogen group spanned a range of divergences. Conserved loci were more likely to catch more divergent species that might not have been present in our initial dataset. For example, we recovered multiple species of *Bartonella* that were not present in our probe set, for which related genomes were available. However, for *Ralstonia* and *Paraburkholderia* species, we identified these samples from reads targeted by probes for the genus *Burkholderia*, a pathogenic taxon in the same family (Burkholderaceae). The ability to identify taxa at these distances is because of the more conserved loci targeted by the bait panel.

During the initial read classification stage, we identified low levels of *Plasmodium* species in all but 2 museum samples, which was unexpected. Museum

samples contained  $\leq 3,221$  *Plasmodium* reads/sample (mean 428.3 reads/sample), but we were unable to assemble them into loci for phylogenetic analyses. This limitation effectively removed those samples from downstream analyses. The *P. falciparum* genome is extremely AT rich (82%, 44), which might result in bioinformatic false-positive results. We suspect that AT-rich, low-complexity regions of the host genome are misclassified as parasite reads. To test this hypothesis, we used fqtrim 0.9.7 (<https://ccb.jhu.edu/software/fqtrim>) to identify and remove low-complexity sequences within those reads. This filter by itself reduced the number of *Plasmodium* reads in the museum samples by 75.5% (maximum 298 reads, mean 57.2 reads). In comparison, only 8.2% of reads from 0.001% enriched control samples and 0.2% of reads from 1% enriched control samples were removed.

Several technical issues still need to be addressed. First, enrichment increases the targeted



- |             |              |              |             |                             |
|-------------|--------------|--------------|-------------|-----------------------------|
| 1. TK136222 | 6. TK164683  | 11. TK164728 | 16. TK48533 | 21. TK49732                 |
| 2. TK136240 | 7. TK164686  | 12. TK179690 | 17. TK49668 | 22. TK49733                 |
| 3. TK154677 | 8. TK164689  | 13. TK185677 | 18. TK49674 | 23. Control enriched 0.001% |
| 4. TK154685 | 9. TK164702  | 14. TK197046 | 19. TK49686 | 24. Control 1%              |
| 5. TK154687 | 10. TK164714 | 15. TK199855 | 20. TK49712 |                             |

**Figure 9.** Genetic identification of mammal host from unenriched, mitochondrial reads in study of prospecting for zoonotic pathogens by using targeted DNA enrichment. Reads were compared with a database of mammalian mitochondria and assigned a taxonomic classification based on these results. A heatmap of the results shows the relative proportion of classified reads assigned to mammalian genera. Samples with <50 mitochondrial reads and single-read genera are not shown.

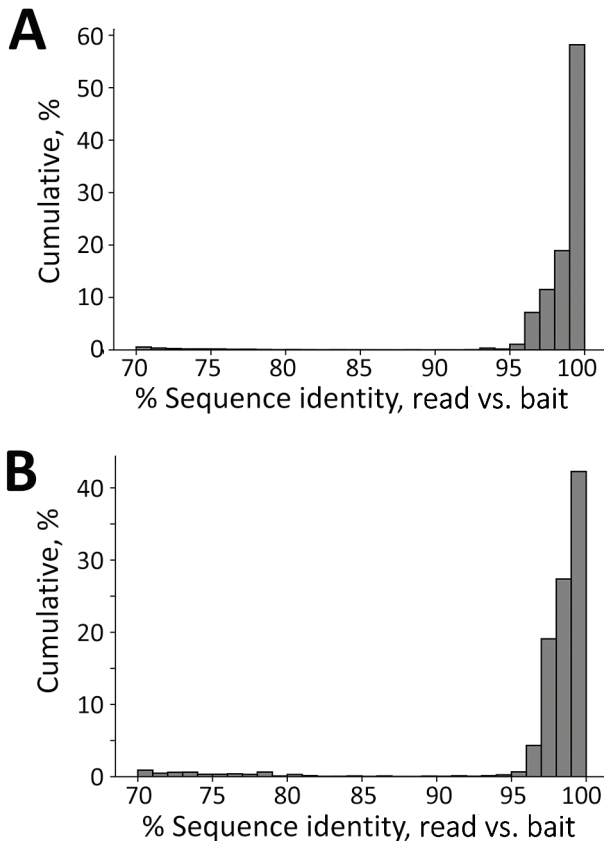


**Figure 10.** Sequence identity between enriched reads and baits in the probe panel used for targeting zoonotic pathogens in study of prospecting for zoonotic pathogens by using targeted DNA enrichment. Reads from each sample were classified against a database of target loci. Sequence identity between pathogen-derived reads and the most similar bait in the bait panel for all pathogens excluding *Bartonella* species (A) and for only *Bartonella* species (B). *Bartonella* was the most common pathogen in our samples, and the number of reads was biased toward a few individuals.

loci coverage by 3 orders of magnitude. However, the amount of host DNA remaining in each sample is still high. Ideally, host DNA would be rare or absent. Second, the bait panel requires relatively large up-front costs. Third, although the bait panel is developed to target a wide range of taxa, it is not possible to know which species are missed. The best way to circumvent that issue is to use controls spiked with various pathogens of interest, similar to how mock communities are used in other metagenomic studies (45). Those mock controls are commercially available for bacterial communities (e.g., ZymoBIOMICS Microbial Community Standards; Zymo Research, <http://www.zymoresearch.com>), but we have been unable to find similar products that contain eukaryotic pathogens. Solutions to those problems will make

targeted sequencing with bait panels a viable tool for pathogen surveillance. Fourth, the sensitivity of the probes will depend on the sequence divergence between the probes and pathogen DNA. The more diverged the 2 are, the less efficient the capture will be. This limitation indicates that pathogen groups that have biased or limited genomic data will be less likely to capture off-target species once divergence increases by >5%–10%. Finally, the current probe panel is capable of capturing and identifying pathogens if there are  $\geq 3,000$  genome copies in the sample. Sensitivity needs to be improved in future iterations of the panel. One method could be to target pathogen-specific, repetitive sequences (46). Because those sequences are already present in the genome hundreds to thousands of times, it should be possible to greatly increase the sensitivity of the probe panel.

Although further effort is required to resolve these issues, we believe that enrichment of pathogen DNA from museum tissue samples is a viable tool worth further development. In its current form, enrichment represents a coarse tool that can be used to scan for various pathogens from archived tissues. More refined tests, such as quantitative PCR and targeted sequencing, can be used to answer taxon-specific questions. Target enrichment will be necessary for maximizing the pathogen data that are available from the hundreds of thousands of museum-archived tissues and will play a critical role in understanding our susceptibility to future zoonotic outbreaks.

#### Acknowledgments

We thank Sandy Smith, John Heaner, Larry Schlesinger, Ian Cheeseman, and Frederic Chevalier for providing computational and laboratory support and Kathy McDonald, Heath Garner, and Caleb Phillips for providing small mammal tissues.

This study was supported by the Texas Biomedical Research Forum (grant 19-04773).

#### About the Author

Dr. Enabulele is a postdoctoral research associate at the Texas Biomedical Research Institute, San Antonio, TX. His primary research interests are public health parasitology, neglected tropical diseases, and pathogen genomics.

#### References

1. Ploverright RK, Parrish CR, McCallum H, Hudson PJ, Ko AI, Graham AL, et al. Pathways to zoonotic spillover. *Nat Rev Microbiol.* 2017;15:502–10. <https://doi.org/10.1038/nrmicro.2017.45>

2. Dean DJ, Evans WM, McClure RC. Pathogenesis of rabies. *Bull World Health Organ.* 1963;29:803–11.
3. Perry RD, Fetherston JD. *Yersinia pestis* – etiologic agent of plague. *Clin Microbiol Rev.* 1997;10:35–66. <https://doi.org/10.1128/CMR.10.1.35>
4. Leroy EM, Epelboin A, Mondonge V, Pourrut X, Gonzalez J-P, Muyembe-Tamfum J-J, et al. Human Ebola outbreak resulting from direct exposure to fruit bats in Luebo, Democratic Republic of Congo, 2007. *Vector Borne Zoonotic Dis.* 2009;9:723–8. <https://doi.org/10.1089/vbz.2008.0167>
5. Petersen JM, Schriefer ME. Tularemia: emergence/re-emergence. *Vet Res.* 2005;36:455–67. <https://doi.org/10.1051/vetres:2005006>
6. Müller B, Dürr S, Alonso S, Hattendorf J, Laise CJ, Parsons SD, et al. Zoonotic *Mycobacterium bovis*-induced tuberculosis in humans. *Emerg Infect Dis.* 2013;19:899–908. <https://doi.org/10.3201/eid1906.120543>
7. Jo WK, de Oliveira-Filho EF, Rasche A, Greenwood AD, Osterrieder K, Drexler JF. Potential zoonotic sources of SARS-CoV-2 infections. *Transbound Emerg Dis.* 2021;68:1824–34. <https://doi.org/10.1111/tbed.13872>
8. van Aart AE, Velkers FC, Fischer EA, Broens EM, Egberink H, Zhao S, et al. SARS-CoV-2 infection in cats and dogs in infected mink farms. *Transbound Emerg Dis.* 2022;69:3001–7. <https://doi.org/10.1111/tbed.14173>
9. Colella JP, Bates J, Burneo SF, Camacho MA, Carrion Bonilla C, Constable I, et al. Leveraging natural history biorepositories as a global, decentralized, pathogen surveillance network. *PLoS Pathog.* 2021;17:e1009583. <https://doi.org/10.1371/journal.ppat.1009583>
10. McLean BS, Bell KC, Dunnum JL, Abrahamson B, Colella JP, Deardorff ER, et al. Natural history collections-based research: progress, promise, and best practices. *J Mammal.* 2016;97:287–97. <https://doi.org/10.1093/jmammal/gyv178>
11. Cook JA, Arai S, Armien B, Bates J, Bonilla CA, Cortez MB, et al. Integrating biodiversity infrastructure into pathogen discovery and mitigation of emerging infectious diseases. *Bioscience.* 2020;70:531–4. <https://doi.org/10.1093/biosci/biaa064>
12. Dunnum JL, Yanagihara R, Johnson KM, Armien B, Batsaikhan N, Morgan L, et al. Biospecimen repositories and integrated databases as critical infrastructure for pathogen discovery and pathobiology research. *PLoS Negl Trop Dis.* 2017;11:e0005133. <https://doi.org/10.1371/journal.pntd.0005133>
13. Thompson CW, Phelps KL, Allard MW, Cook JA, Dunnum JL, Ferguson AW, et al. Preserve a voucher specimen! The critical need for integrating natural history collections in infectious disease studies. *MBio.* 2021;12:e02698–20. <https://doi.org/10.1128/mBio.02698-20>
14. Soniat TJ, Sihaloho HF, Stevens RD, Little TD, Phillips CD, Bradley RD. Temporal-dependent effects of DNA degradation on frozen tissues archived at –80°C. *J Mammal.* 2021;102:375–83. <https://doi.org/10.1093/jmammal/gyab009>
15. Yates TL, Mills JN, Parmenter CA, Ksiazek TG, Parmenter RR, Vande Castle JR, et al. The ecology and evolutionary history of an emergent disease: hantavirus pulmonary syndrome. Evidence from two El Niño episodes in the American southwest suggests that El Niño-driven precipitation, the initial catalyst of a trophic cascade that results in a delayed density-dependent rodent response, is sufficient to predict heightened risk for human contraction of hantavirus pulmonary syndrome. *Bioscience.* 2002;52:989–98. [https://doi.org/10.1641/0006-3568\(2002\)052\[0989:TEAEHO\]2.0.CO;2](https://doi.org/10.1641/0006-3568(2002)052[0989:TEAEHO]2.0.CO;2)
16. Choi M, Scholl UI, Ji W, Liu T, Tikhonova IR, Zumbo P, et al. Genetic diagnosis by whole exome capture and massively parallel DNA sequencing. *Proc Natl Acad Sci U S A.* 2009;106:19096–101. <https://doi.org/10.1073/pnas.0910672106>
17. Yi X, Liang Y, Huerta-Sanchez E, Jin X, Cuo ZX, Pool JE, et al. Sequencing of 50 human exomes reveals adaptation to high altitude. *Science.* 2010;329:75–8. <https://doi.org/10.1126/science.1190371>
18. McCormack JE, Hird SM, Zellmer AJ, Carstens BC, Brumfield RT. Applications of next-generation sequencing to phylogeography and phylogenetics. *Mol Phylogenet Evol.* 2013;66:526–38. <https://doi.org/10.1016/j.ympev.2011.12.007>
19. Vernot B, Zavala EI, Gómez-Olivencia A, Jacobs Z, Slon V, Mafessoni F, et al. Unearthing Neanderthal population history using nuclear and mitochondrial DNA from cave sediments. *Science.* 2021;372:eabf1667. <https://doi.org/10.1126/science.abf1667>
20. Fu Q, Hajdinjak M, Moldovan OT, Constantin S, Mallick S, Skoglund P, et al. An early modern human from Romania with a recent Neanderthal ancestor. *Nature.* 2015;524:216–9. <https://doi.org/10.1038/nature14558>
21. Gaudin M, Desnues C. Hybrid capture-based next generation sequencing and its application to human infectious diseases. *Front Microbiol.* 2018;9:2924. <https://doi.org/10.3389/fmicb.2018.02924>
22. Keller M, Spyrou MA, Scheib CL, Neumann GU, Kröpelin A, Haas-Gebhard B, et al. Ancient *Yersinia pestis* genomes from across Western Europe reveal early diversification during the First Pandemic (541–750). *Proc Natl Acad Sci U S A.* 2019;116:12363–72. <https://doi.org/10.1073/pnas.1820447116>
23. Lee JS, Mackie RS, Harrison T, Shariat B, Kind T, Kehl T, et al. Targeted enrichment for pathogen detection and characterization in three felid species. *J Clin Microbiol.* 2017;55:1658–70. <https://doi.org/10.1128/JCM.01463-16>
24. Wylie TN, Wylie KM, Herter BN, Storch GA. Enhanced virome sequencing using targeted sequence capture. *Genome Res.* 2015;25:1910–20. <https://doi.org/10.1101/gr.191049.115>
25. O’Flaherty BM, Li Y, Tao Y, Paden CR, Queen K, Zhang J, et al. Comprehensive viral enrichment enables sensitive respiratory virus genomic identification and analysis by next generation sequencing. *Genome Res.* 2018;28:869–77. <https://doi.org/10.1101/gr.226316.117>
26. Faircloth BC, McCormack JE, Crawford NG, Harvey MG, Brumfield RT, Glenn TC. Ultraconserved elements anchor thousands of genetic markers spanning multiple evolutionary timescales. *Syst Biol.* 2012;61:717–26. <https://doi.org/10.1093/sysbio/sys004>
27. Faircloth BC. Identifying conserved genomic elements and designing universal bait sets to enrich them. *Methods Ecol Evol.* 2017;8:1103–12. <https://doi.org/10.1111/2041-210X.12754>
28. Gotia HT, Munro JB, Knowles DP, Daubenberger CA, Bishop RP, Silva JC. Absolute quantification of the host-to-parasite DNA ratio in *Theileria parva*-infected lymphocyte cell lines. *PLoS One.* 2016;11:e0150401. <https://doi.org/10.1371/journal.pone.0150401>
29. Cowell AN, Loy DE, Sundaraman SA, Valdivia H, Fisch K, Lescano AG, et al. Selective whole-genome amplification is a robust method that enables scalable whole-genome sequencing of from unprocessed clinical samples. *MBio.* 2017;8:e02257-16. <https://doi.org/10.1128/mBio.02257-16>
30. Bushnell B. BBMap: a fast, accurate, splice-aware aligner. Berkeley (CA): Lawrence Berkeley National Laboratory; 2014.

31. Wood DE, Lu J, Langmead B. Improved metagenomic analysis with Kraken 2. *Genome Biol.* 2019;20:257. <https://doi.org/10.1186/s13059-019-1891-0>
32. Bankevich A, Nurk S, Antipov D, Gurevich AA, Dvorkin M, Kulikov AS, et al. SPAdes: a new genome assembly algorithm and its applications to single-cell sequencing. *J Comput Biol.* 2012;19:455–77. <https://doi.org/10.1089/cmb.2012.0021>
33. Kozlov AM, Darriba D, Flouri T, Morel B, Stamatakis A. RAxML-NG: a fast, scalable and user-friendly tool for maximum likelihood phylogenetic inference. *Bioinformatics.* 2019;35:4453–5. <https://doi.org/10.1093/bioinformatics/btz305>
34. Jacomo V, Kelly PJ, Raoult D. Natural history of *Bartonella* infections (an exception to Koch's postulate). *Clin Diagn Lab Immunol.* 2002;9:8–18.
35. Chomel BB, Boulouis HJ, Maruyama S, Breitschwerdt EB. *Bartonella* spp. in pets and effect on human health. *Emerg Infect Dis.* 2006;12:389–94. <https://doi.org/10.3201/eid1203.050931>
36. Dahmani M, Diatta G, Labas N, Diop A, Bassene H, Raoult D, et al. Noncontiguous finished genome sequence and description of *Bartonella mastomydis* sp. nov. *New Microbes New Infect.* 2018;25:60–70. <https://doi.org/10.1016/j.nmni.2018.03.005>
37. Briese T, Kapoor A, Mishra N, Jain K, Kumar A, Jabado OJ, et al. Virome capture sequencing enables sensitive viral diagnosis and comprehensive virome analysis. *MBio.* 2015;6:e01491–15. <https://doi.org/10.1128/mBio.01491-15>
38. Gerrits GP, Klaassen C, Coenye T, Vandamme P, Meis JF. *Burkholderia fungorum* septicemia. *Emerg Infect Dis.* 2005;11:1115–7. <https://doi.org/10.3201/eid1107.041290>
39. Vandamme P, Peeters C. Time to revisit polyphasic taxonomy. *Antonie van Leeuwenhoek.* 2014;106:57–65. <https://doi.org/10.1007/s10482-014-0148-x>
40. Angus AA, Agapakis CM, Fong S, Yerrapragada S, Estrada-de los Santos P, Yang P, et al. Plant-associated symbiotic *Burkholderia* species lack hallmark strategies required in mammalian pathogenesis. *PLoS One.* 2014;9:e83779. <https://doi.org/10.1371/journal.pone.0083779>
41. Salter SJ, Cox MJ, Turek EM, Calus ST, Cookson WO, Moffatt MF, et al. Reagent and laboratory contamination can critically impact sequence-based microbiome analyses. *BMC Biol.* 2014;12:87. <https://doi.org/10.1186/s12915-014-0087-z>
42. Chen YY, Huang WT, Chen CP, Sun SM, Kuo FM, Chan YJ, et al. An outbreak of *Ralstonia pickettii* bloodstream infection associated with an intrinsically contaminated normal saline solution. *Infect Control Hosp Epidemiol.* 2017;38:444–8. <https://doi.org/10.1017/ice.2016.327>
43. Bi K, Vanderpool D, Singhal S, Linderoth T, Moritz C, Good JM. Transcriptome-based exon capture enables highly cost-effective comparative genomic data collection at moderate evolutionary scales. *BMC Genomics.* 2012;13:403. <https://doi.org/10.1186/1471-2164-13-403>
44. Weber JL. Analysis of sequences from the extremely A + T-rich genome of *Plasmodium falciparum*. *Gene.* 1987;52:103–9. [https://doi.org/10.1016/0378-1119\(87\)90399-4](https://doi.org/10.1016/0378-1119(87)90399-4)
45. Tourlousse DM, Narita K, Miura T, Ohashi A, Matsuda M, Ohyama Y, et al. Characterization and demonstration of mock communities as control reagents for accurate human microbiome community measurements. *Microbiol Spectr.* 2022;10:e0191521. <https://doi.org/10.1128/spectrum.01915-21>
46. Bennuru S, O'Connell EM, Drame PM, Nutman TB. Mining filarial genomes for diagnostic and therapeutic targets. *Trends Parasitol.* 2018;34:80–90. <https://doi.org/10.1016/j.pt.2017.09.003>

---

Address for correspondence: Roy N. Platt, Texas Biomedical Research Institute, 8715 W Military Dr, San Antonio, TX 78245-0549, USA; email: rplatt@txbiomed.org

*EID cannot ensure accessibility for Supplemental Materials supplied by authors. Readers who have difficulty accessing supplementary content should contact the authors for assistance.*

# Prospecting for Zoonotic Pathogens by Using Targeted DNA Enrichment

## Appendix 1

### Materials and Methods

#### Host-Pathogen Control Samples

We isolated DNA using the QIAGEN blood and tissue kit following manufacturer's protocol and quantified DNA using Qubit. We prepared a cocktail of pathogen DNA mixtures comprising 200 ng DNA of each pathogen (*Mycobacterium bovis*, *M. tuberculosis*, *Plasmodium vivax*, *P. falciparum*, *Schistosoma mansoni*, and *S. bovis*). A mammalian-pathogen DNA mixture was prepared by mixing pathogen DNA in DNA from uninfected liver tissues of laboratory mouse (*Mus musculus*) to make 1% and 0.001% pathogen mixtures. The negative control was prepared from the same uninfected liver tissues of laboratory mouse (*Mus musculus*) without spiking with pathogens.

#### Museum-Archived Samples and Controls

We extracted DNA from 42 museum samples comprising of mammalian liver tissues (in lysed buffer or frozen in liquid nitrogen) collected between 1995 and 2018 in Africa, Southern America, and the United States. Control samples were as previously described (1% and 0.001% pathogens DNA in mammalian DNA). Information for each specimen are provided in Table 2.

#### Computing Environment and Reproducibility

All analyses were performed on a single compute node with 48 processors and limited to 100 Gb of RAM. Bioinformatic steps were documented in a series of BASH shell scripts or Jupyter v4.9.2 notebooks. These files along with conda v4.11.0 environments are available ([github.com/nealplatt/pathogen\\_probes](https://github.com/nealplatt/pathogen_probes)) and are archived: DOI:10.5281/zenodo.7319915.

## Panel Development

We developed a set of biotinylated probes for UCE-based, targeted sequencing of 32 pathogen groups (Table 1). For example, given the large evolutionary distances covered by various pathogens, we generated sets of probes that target more discrete taxonomic groups (e.g., Nematoda, *Yersinia*). For bacterial pathogens, probes were designed to capture all species within the genus or species group. For eukaryotic pathogens, probes were designed to be effective at taxonomic ranks that ranged from species group to class. The taxonomic rank varied in eukaryotic pathogens based on the following criteria: 1) the number of available genomes, 2) sequence diversity - because this impacted the number of probes needed. Table 1 provides information on the pathogen group, targeted zoonotic agent and zoonoses.

For each group we used the Phyluce package v1.7.0 (1,2); we generated probes to target  $\approx 49$  loci using the methods described below. First, we identified orthologous loci between a focal pathogen and the remaining species in the pathogen group. Focal taxa were chosen based on their assembly contiguity or prominence as a zoonotic agent. To do this we downloaded a genome for each species in the pathogen group. Accession numbers for these assemblies are provided in Table 2. Next, we simulated 25x read coverage for each genome using the ART v2016.06.05 (3); read simulator with the following options: `art_illumina-paired-len 100-fcov 25-mflen 200-sdev 150 -ir 0.0 -ir2 0.0 -dr 0.0 -dr2 0.0 -qs 100 -qs2 100 -na`. Simulated reads from all query taxa were mapped back to a focal taxon with `bbmap v38.93` (4); enabling up to 10% sequence divergence (`minid = 0.9`). Unmapped, or multimapping reads were removed using `Bedtools v2.9.2` (5) and `phyluce_probe_strip_masked_loci_from_set (filter_mask 25%)`. The remaining reads were merged to generate a BED file containing orthologous regions between the query and focal taxa.

Then, we identified orthologous loci among all taxa within the pathogen group using `phyluce_probe_query_multi_merge_table`. Next, we filtered each set of loci to retain only those shared among 33% of taxa in the pathogen group using `phyluce_probe_query_multi_merge_table`. We extracted 160 bp from each locus and generated an initial set of in silico probes directly from the focal genome using `phyluce_probe_get_genome_sequences_from_bed` and `phyluce_probe_get_tiled_probes`. Additional options for probe design included generating two probes per locus (`-two_probes`) that overlapped in the middle (`-overlap-middle`). Focal probes with repetitive regions or skewed GC



content (<30% or >70%) content were removed. Next, the probes from the focal taxa were mapped back to each genome in the pathogen group with `phyluce_probe_run_multiple_lastzs_sqlite`. We used the `-identity` option to limit searches with a maximum divergence of 30%. Using these results, we extracted 120-bp loci from the probed regions in each representative genome extracted using `phyluce_probe_slice_sequence_from_genomes`. Theoretically, this dataset should contain orthologous 120-bp sequences from most taxa in each pathogen group. We verified this with `phyluce_probe_get_multi_fasta_table`, which provides a table showing the number of taxa identified at each locus. We used this information to identify the 100 loci capable of capturing most taxa from the pathogen group. Next, we generated two 80-bp probes from each of the 100-bp and 120-bp loci. We used `phyluce_probe_easy_lastz` to compare the probes to themselves and remove any that were possible duplicates. Then we reduced the probe set even further by clustering probes based on sequence identity with `cd-hit-est v4.8.1` (6). We identified sequence clusters with >95% similarity and retained only 1 probe per group. Finally, we recalculated the number of probes needed to capture each locus.

The proceeding steps were repeated for each pathogen group shown in Table 1. To generate a final panel, we selected 49 loci per pathogen group in a way that minimized the number of probes needed. In some cases, we needed to generate 2 sets of probes to adequately represent target pathogens. For example, Kinetoplastea contains 2 pathogens of interest, *Trypanosoma* and *Leishmania*. The baits designed for *Leishmania* were able to target all 49 loci in the most of the Kinetoplastea but only 23 loci in *Trypanosoma*. We then generated a second set of 617 *Trypanosoma*-specific baits to augment the kinetoplastid baits and ensure that *Trypanosoma* parasites were represented adequately in the final panel. Likewise, we doubled the number of baits used to capture loci from the *Bacillus cereus* group to effectively capture *B. cereus* and *B. anthracis*. The probe set was quality checked by Arbor Biosciences. This included comparing the probe set to mammal genomes with `blastn v2.12.0` (7) and checking for low-complexity sequences. Any probes that failed quality control were replaced before synthesis.

### **Library Preparation**

Standard DNA sequencing libraries were generated from 500 ng of DNA per sample. We used the KAPA Hyperplus kit protocol with the following modifications: 1) enzymatic fragmentation at 37°C for 10 minutes, 2) adaptor ligation at 20°C for an hour, and 3) four cycles

of library PCR amplification. To minimize adaptor switching we used unique dual indexed (UDI) adaptors (IDT xGen Stubby Adaptor-UDI Primers). Each library was eluted in 20  $\mu\text{L}$  of sterile water and the base pairs sizes and concentration estimated by Agilent 4200 TapeStation (Figure 2).

Individual samples with similar DNA concentrations were combined together into pools of 4–16 samples and the total volume was reduced to 7  $\mu\text{L}$  with a speedvac vacuum concentrator. Next, we used the high sensitivity protocol of myBaits v.5 (Daicel Arbor Biosciences) to enrich target pathogen loci from the host/pathogen control and museum archived samples. We used 2 rounds of enrichment for each pool of samples. Probe concentration was 100 ng/ $\mu\text{L}$ . Each round was 24 hours at 65°C. After washing of unbound DNA, each library was amplified with a 15-cycle PCR amplification step and quantified using qPCR. Finally, the pools of 4–16 were combined into an equimolar pool for sequencing. All sequencing reactions were on single lanes of Illumina Hi-Seq 2500.

### **Bioinformatic Analyses**

All analyses were performed on a single compute node with 48 processors and limited to 100 Gb of RAM. Bioinformatic steps were documented in a series of BASH shell scripts or Jupyter notebooks. These files along with conda environments are available at [github.com/nealplatt/pathogen\\_probes](https://github.com/nealplatt/pathogen_probes) and archived. The basic structure of the bioinformatic analyses are shown in Figure 3. In general, we used the Kraken2 v2.1.2 (8) to assign a taxonomic id to each read, the Phyluce v1.7.1 (1,2) pipeline to identify, assemble, and align loci, and RaxML-NG v1.0.1 to generate phylogenies from each pathogen group of interest.

First, we used Trimmomatic v0.39 (9) to trim and quality filter low-quality bases and Illumina adaptors. Then, we used Kraken2 v2.1.1 (8) to compare each read from our samples to a reduced dataset of target loci using a `-conf` cutoff of 0.2. We decided to compare our reads to a reduced dataset of target loci to minimize the computational expense of these comparison. To generate the reduced database of bait-targeted loci, we downloaded one representative or reference genome from all species in RefSeq v212 (10) with `genome_updater.sh` v0.5.1 ([https://github.com/pirovc/genome\\_updater](https://github.com/pirovc/genome_updater)). Then we used BMAP v38.96 (4) to map all the baits to each genome and kept the 10 best sites that mapped with  $\geq 85\%$  sequence identity.

Next, we extracted these hits along with 1,000 bp up and downstream. These sequences were combined into a single fasta file that should contain the major mapping locations for our baits.

Once reads were classified we identified genera that were known pathogens or were present in at least one sample with more than 1,000 reads. Next, we extracted reads from the relevant family with KrakenTools v1.2 (<https://github.com/jenniferlu717/KrakenTools/>). These reads were then assembled (Figure 3, panel B) with the SPAdes genome assembler v3.14.1 (11) using the `phyluce_assembly_assemblo_spades` wrapper script. We filtered out low quality contigs based on size (<100 bp) and median coverage (<10×) as calculated by the SPAdes genome assembler. Next, we filtered individuals even further by removing individuals with fewer <2 contigs.

While we were assembling and filtering contigs from each isolated target loci from species with available genome assemblies, we used `genome_updater.sh` v0.5.1 ([https://github.com/pirovc/genome\\_updater](https://github.com/pirovc/genome_updater)) to download one (-A 1) reference or representative (-c reference genome, representative genome) genome from either refseq or Genbank (-d refseq.genbank) for the pathogen group. We also included at least 1 individual from an outlier genus to root downstream analyses. These genomes were converted to twobit format with `faToTwoBit`. Next, we used `phyluce_probe_run_multiple_lastzs_sqlite` to compare probes from the pathogen group to the genome assemblies with an identity cut off of 85% (-identity 0.85). These loci plus 1 kb of flanking sequence (-flank 1000) were extracted from the genome using `phyluce_probe_slice_sequence_from_genomes`. After extraction, the sliced loci were identified and counted using `phyluce_assembly_match_contigs_to_probes` (-min-identity 90) and `phyluce_assembly_get_match_counts`. Next, we combined the loci generated from our samples with those from representative and reference genomes and aligned them with `phyluce_align_seqcap_align`. The resulting alignments were trimmed with `gblocks` v0.91b (12) and `phyluce_align_get_gblocks_trimmed_alignments_from_untrimmed`. We then counted the number of taxa per locus alignment (`phyluce_align_get_taxon_locus_counts_in_alignments`) and removed taxa with fewer than 2 loci (`phyluce_align_extract_taxa_from_alignments`). Then we removed any loci that contain fewer than half of the expected number of taxa with `phyluce_align_get_only_loci_with_min_taxa` and concatenated the remaining loci into a single phylip alignment (`phyluce_align_concatenate_alignments`).

We used RaxML-NG v1.0.1 (13) to generate a maximum-likelihood phylogenetic tree from the concatenated alignment. We ran 100 parsimony tree searches and then another 1,000 replicates using the GTR + G substitution model. Branches with less than 50% support were collapsed with the Newick Utilities v1.6 (14), Newick editor (nw\_ed <input\_tree\_file>'i and b< = 50'). These steps were then repeated with other pathogen groups identified in the samples.

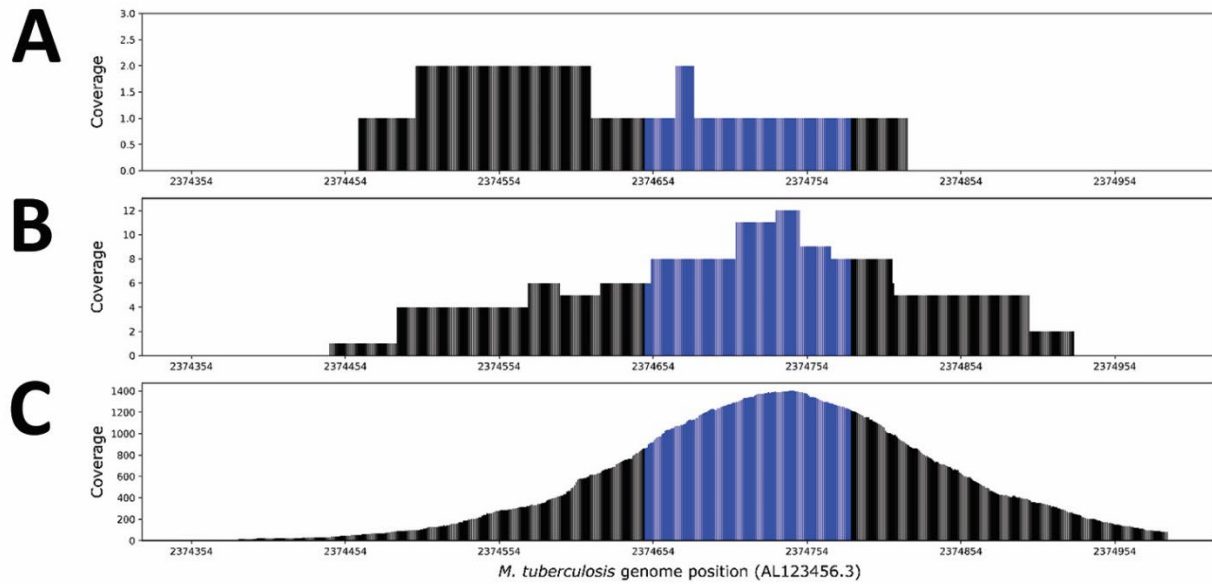
### Host Identification

We verified museum identifications by comparing reads to a second Kraken2 v2.1.2 (8) database containing mammalian mitochondrial genomes. To do this, we downloaded all available mammalian mitochondrial genomes (n = 1,651) from <https://www.ncbi.nlm.nih.gov/genome/organelle/> (last accessed 3 November 2022). We then created a custom database and compared each of our samples using Kraken2 and no confidence cutoffs. The Kraken2 classifications were filtered by removing any samples with fewer than 50 classified reads and any single-read, generic classifications.

### References

1. Faircloth BC, McCormack JE, Crawford NG, Harvey MG, Brumfield RT, Glenn TC. Ultraconserved elements anchor thousands of genetic markers spanning multiple evolutionary timescales. *Syst Biol.* 2012;61:717–26. [PubMed https://doi.org/10.1093/sysbio/sys004](https://doi.org/10.1093/sysbio/sys004)
2. Faircloth BC. Identifying conserved genomic elements and designing universal bait sets to enrich them. *Methods Ecol Evol.* 2017;8:1103–12. <https://doi.org/10.1111/2041-210X.12754>
3. Huang W, Li L, Myers JR, Marth GT. ART: a next-generation sequencing read simulator. *Bioinformatics.* 2012;28:593–4. [PubMed https://doi.org/10.1093/bioinformatics/btr708](https://doi.org/10.1093/bioinformatics/btr708)
4. Bushnell B. BBMap: a fast, accurate, splice-aware aligner. Berkeley (CA): Lawrence Berkeley National Laboratory; 2014.
5. Quinlan AR, Hall IM. BEDTools: a flexible suite of utilities for comparing genomic features. *Bioinformatics.* 2010;26:841–2. [PubMed https://doi.org/10.1093/bioinformatics/btq033](https://doi.org/10.1093/bioinformatics/btq033)
6. Fu L, Niu B, Zhu Z, Wu S, Li W. CD-HIT: accelerated for clustering the next-generation sequencing data. *Bioinformatics.* 2012;28:3150–2. [PubMed https://doi.org/10.1093/bioinformatics/bts565](https://doi.org/10.1093/bioinformatics/bts565)
7. Altschul SF, Gish W, Miller W, Myers EW, Lipman DJ. Basic local alignment search tool. *J Mol Biol.* 1990;215:403–10. [PubMed https://doi.org/10.1016/S0022-2836\(05\)80360-2](https://doi.org/10.1016/S0022-2836(05)80360-2)

8. Wood DE, Lu J, Langmead B. Improved metagenomic analysis with Kraken 2. *Genome Biol.* 2019;20:257. [PubMed https://doi.org/10.1186/s13059-019-1891-0](https://doi.org/10.1186/s13059-019-1891-0)
9. Bolger AM, Lohse M, Usadel B. Trimmomatic: a flexible trimmer for Illumina sequence data. *Bioinformatics.* 2014;30:2114–20. [PubMed https://doi.org/10.1093/bioinformatics/btu170](https://doi.org/10.1093/bioinformatics/btu170)
10. O’Leary NA, Wright MW, Brister JR, Ciuffo S, Haddad D, McVeigh R, et al. Reference sequence (RefSeq) database at NCBI: current status, taxonomic expansion, and functional annotation. *Nucleic Acids Res.* 2016;44(D1):D733–45. [PubMed https://doi.org/10.1093/nar/gkv1189](https://doi.org/10.1093/nar/gkv1189)
11. Bankevich A, Nurk S, Antipov D, Gurevich AA, Dvorkin M, Kulikov AS, et al. SPAdes: a new genome assembly algorithm and its applications to single-cell sequencing. *J Comput Biol.* 2012;19:455–77. [PubMed https://doi.org/10.1089/cmb.2012.0021](https://doi.org/10.1089/cmb.2012.0021)
12. Talavera G, Castresana J. Improvement of phylogenies after removing divergent and ambiguously aligned blocks from protein sequence alignments. *Syst Biol.* 2007;56:564–77. [PubMed https://doi.org/10.1080/10635150701472164](https://doi.org/10.1080/10635150701472164)
13. Kozlov AM, Darriba D, Flouri T, Morel B, Stamatakis A. RAxML-NG: a fast, scalable and user-friendly tool for maximum likelihood phylogenetic inference. *Bioinformatics.* 2019;35:4453–5. [PubMed https://doi.org/10.1093/bioinformatics/btz305](https://doi.org/10.1093/bioinformatics/btz305)
14. Junier T, Zdobnov EM. The Newick utilities: high-throughput phylogenetic tree processing in the UNIX shell. *Bioinformatics.* 2010;26:1669–70. [PubMed https://doi.org/10.1093/bioinformatics/btq243](https://doi.org/10.1093/bioinformatics/btq243)



**Appendix Figure.** Read depth at a targeted region in *Mycobacterium tuberculosis* in the A) 1%, unenriched, B) 0.001% enriched, and C) 1% enriched control, samples. This particular probe was designed for (AL123456.3:2,374,648–2,374,781; shown in blue). Median coverage at this locus increased from 1x in the 1% unenriched sample (A) to 8x in the 0.001% enriched sample (B) and 1,278x in the 1% enriched control sample (C).